

CORRESPONDENCE

Open Access

Depletion of giant ANK2 in monkeys causes drastic brain volume loss

Dong-Dong Qin^{1,2}, Jian-Kui Zhou³, Xie-Chao He⁴, Xiang-Yu Shen⁵, Cong Li^{6,7}, Huan-Zhi Chen^{1,7}, Lan-Zhen Yan⁴, Zheng-Fei Hu⁴, Xiang Li⁴, Long-Bao Lv⁴, Yong-Gang Yao^{1,4,7,8,9}, Zheng Wang^{1,5,8}, Xing-Xu Huang¹⁰, Xin-Tian Hu^{1,4,8} and Ping Zheng^{4,6,9,11,12}

Dear Editor,

Autism spectrum disorders (ASDs) are heritable neurodevelopmental disabilities with core symptoms of impaired reciprocal social behaviors and restrictive or repetitive behaviors¹. ASDs are relatively common developmental neuropsychiatric disorders and important public health issues, affecting around 1%–2% of the population². ASDs have been classified into syndromic and nonsyndromic (also called classic or idiopathic). Most syndromic ASDs have a genetic basis and around 1000 candidate risk genes have been identified according to the Simons Foundation Autism Research Initiative (SFARI Gene: <https://www.sfari.org/resource/sfari-gene/>). Unlike syndromic ASDs, the etiologies of most nonsyndromic ASD cases are largely unknown and very limited genes have been implicated in that.

ANK2 is a member of ankryin gene family and is transcribed into two major isoforms via alternative splicing. The two isoforms produce 220 and 440 kDa polypeptides, termed ANK2 and giant ANK2, respectively³. Compared to ANK2, giant ANK2 has an additional fragment encoded by exon 37 (2066 amino acid residues in cynomolgus and rhesus monkeys, and 2085 amino acid residues in human). Unlike ANK2 which displays broad expression in many tissues including nervous system, giant ANK2 is

restrictively expressed in nervous system⁴. Several giant ANK2-specific mutations (p.P1843S, p.R2608 frameshift, and p.E3429V), which locate in exon 37, were identified in nonsyndromic ASD patients⁴. In addition, a recent study of giant ANK2 deletion in mice revealed that loss of giant ANK2 has no effects on brain structure, but displays mild impairment on selected communicative and social behaviors⁴. These studies suggested that giant ANK2 might be a potential genetic factor involved in nonsyndromic ASDs. Although the laboratory mice are widely employed to decipher the molecular and cellular mechanisms underlying ASDs, rodent models have the limitation that the animals are phylogenetically distant from human. Non-human primates share higher degree of similarity with humans in genome sequence and physiology⁵. Specifically, monkeys have a well-developed prefrontal cortex and display a repertoire of behaviors that are more relevant to ASDs⁵. Several recent studies have established reliable syndromic ASDs monkey models by overexpression or knockout of *MECP2* or *SHANK3* in cynomolgus monkeys^{6–8}.

In this study, we evaluated the function of giant ANK2 and its relevance to human nonsyndromic ASDs by using CRISPR/Cas9 gene-edited cynomolgus monkeys (*Macaca fascicularis*) and rhesus monkeys (*Macaca mulatta*) in which giant ANK2 was specifically knocked out whilst ANK2 remained intact. Two sgRNAs were designed to target distinct sites at exon 37 encoding unique fragment of giant ANK2 (Fig. 1a). Evaluating the cynomolgus monkey pre-implantation embryos revealed high editing efficiency (Supplementary Fig. S1). After embryo transfer, we obtained three pregnancies in cynomolgus monkeys and six in rhesus monkeys, respectively. All fetuses developed to full term. Unfortunately, one cynomolgus monkey and three rhesus monkeys died within 17 days

Correspondence: Yong-Gang Yao (yaoyg@mail.kiz.ac.cn) or Zheng Wang (zheng.wang@ion.ac.cn) or Xing-Xu Huang (huangxx@shanghaitech.edu.cn) or Xin-Tian Hu (xthu@mail.kiz.ac.cn) or Ping Zheng (zhengp@mail.kiz.ac.cn)

¹Key Laboratory of Animal Models and Human Disease Mechanisms, Chinese Academy of Sciences and Yunnan Province, Kunming Institute of Zoology, Chinese Academy of Sciences, Kunming, Yunnan, China

²School of Basic Medical Sciences, Yunnan University of Chinese Medicine, Kunming, Yunnan, China

Full list of author information is available at the end of the article

These authors contributed equally: Dong-Dong Qin, Jian-Kui Zhou, Xie-Chao He, Xiang-Yu Shen

© The Author(s) 2021



Open Access This article is licensed under a Creative Commons Attribution 4.0 International License, which permits use, sharing, adaptation, distribution and reproduction in any medium or format, as long as you give appropriate credit to the original author(s) and the source, provide a link to the Creative Commons license, and indicate if changes were made. The images or other third party material in this article are included in the article's Creative Commons license, unless indicated otherwise in a credit line to the material. If material is not included in the article's Creative Commons license and your intended use is not permitted by statutory regulation or exceeds the permitted use, you will need to obtain permission directly from the copyright holder. To view a copy of this license, visit <http://creativecommons.org/licenses/by/4.0/>.

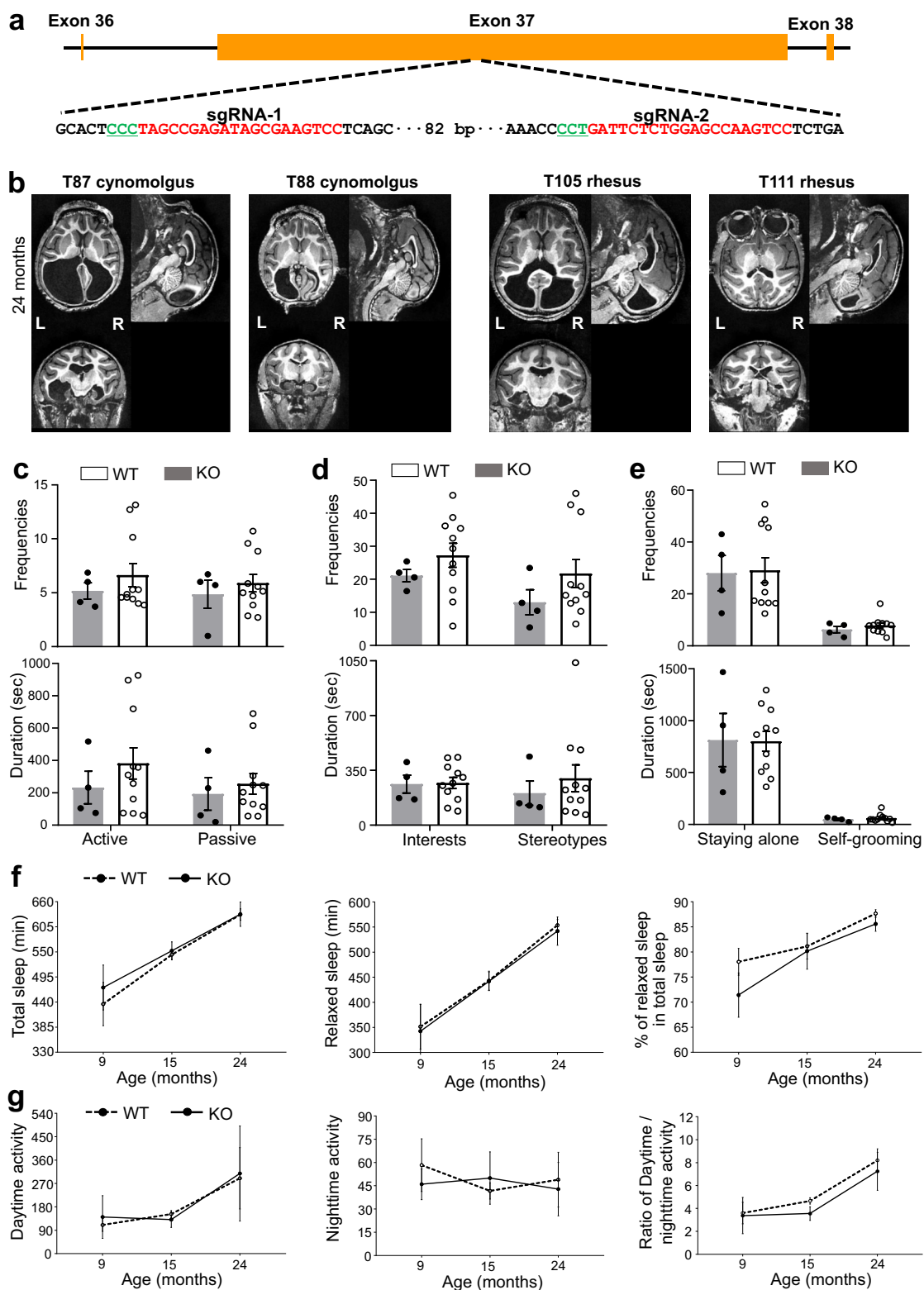


Fig. 1 (See legend on next page.)

(see figure on previous page)

Fig. 1 Giant ANK2 knockout monkeys display reproducible brain volume loss, but do not show ASDs symptoms and have normal sleep–wake cycle. **a** Schematic diagram showing two sgRNAs which target the specific exon of giant ANK2. **b** Example axial, sagittal, and coronal slices of structural images of each knockout (KO) monkey at 24-month. L-left; R-right. **c–e** Frequencies and durations of both active and passive social interaction (**c**), exploratory and stereotypical behaviors (**d**), staying alone and self-grooming (**e**) between KO and WT monkeys. **f, g** No significant difference of the sleep state (**f**) (including the duration of total sleep and relaxed sleep, and the percentage of relaxed sleep in total sleep) and the activity (**g**) (including day-time activity, night-time activity and ratio of day-time/night-time activity) between KO and WT monkeys. All data in (**c–g**) were presented as means \pm SEM.

after birth. Genotyping of the nine monkeys was conducted using genomic DNA extracted from the umbilical cord, ear skin, or blood samples (Supplementary Table S1). Among the five live monkeys, two cynomolgus monkeys and two rhesus monkeys contained frame-shift mutations at both alleles (Supplementary Fig. S2 and Table S1). These frame-shift mutations caused premature translational stop and possibly a complete loss of the functional giant ANK2. Notably, one rhesus monkey (T113) harbored only a small fragment deletion and missense mutations (Supplementary Fig. S2a), which may not significantly alter giant ANK2 functions. We collected eight different tissues from dead monkeys and confirmed the mutations by using Sanger sequencing (Supplementary Fig. S3). We also validated the mutations of *ANK2* at both alleles in brain or liver tissue from three dead monkeys and in peripheral blood samples from all five live monkeys with successful genetic modification using the second-generation sequencing technologies (Supplementary Figs. S2b, S3, and S4). Furthermore, we examined the protein expression of ANK2 and giant ANK2 in the brain of one dead monkey (T114, frameshift). Due to the extremely large size of giant ANK2 (~440 kDa), we had difficulty in detecting this isoform in wild-type (WT) control. However, we confirmed that the ANK2 isoform (~220 kDa) was not affected in knockout (KO) monkey (Supplementary Fig. S2c), demonstrating the specific mutation of giant ANK2 isoform.

We firstly examined the possible influence of giant ANK2 mutation on brain structures. WT monkeys with matched ages and growth conditions were used as controls and were raised together with the mutant monkeys (Supplementary Table S1). Magnetic resonance imaging (MRI) scanning of monkey brains was performed using a United Imaging UMR 790 3T scanner (Shanghai, China) when monkeys were 6-month, 12-month, and 24-month old. Notably, a drastic brain structure change predicting the enlargement of lateral ventricles was reproducibly detected in two cynomolgus monkeys (T87 and T88) and two rhesus monkeys (T105 and T111), all of which carried frame-shift mutations and premature translational stop of giant ANK2. Moreover, the structural alternations were persistent at all examined ages. Some MRI scanning results were shown for the 24-month (Fig. 1b) and other ages as well (Supplementary Fig. S5a, b). Notably, the

mutant rhesus monkey (T113) carrying only small fragment deletion and missense mutations did not display detectable brain structural abnormality compared to WT control (Supplementary Fig. S5c). This could be attributed to the mild change of protein sequence which may not alter protein functions. We therefore exclude this monkey (T113) from the following analyses.

Next, we conducted a quantitative analysis on structural MRI data that were collected at 24-month to evaluate the brain volumetric alterations. Each monkey's brain was registered and segmented into 94 sub-regions based on the brain atlases of rhesus macaque (F99) and cynomolgus macaque (Cyno162)^{9,10}. The structural MRI data for each mutant monkey was compared with specie-specific standard brain atlas instead of species-matched WT controls in this study, as these standard brain atlases were constructed by using more WT individuals^{9,10}. The loss of gray matter volume (GMV) in each brain region was defined as the percentage of missing GMV (dark signal in T1-weighted MRI images) compared to the specie-specific standard brain atlas, i.e., dividing the missing GMV volume by the standardized regional GMV of the brain atlases^{9,10}. The total brain volume of individuals was normalized by the total volume of the atlas. The average percentages of regional GMV loss for each brain region throughout the whole brain were shown (Supplementary Fig. S6a). The distribution of regional GMV loss in individual mutant monkeys was plotted as a violin plot (Supplementary Fig. S6b), and the top 20 brain regions with the largest GMV loss in mutant monkeys compared to WT controls were listed (Supplementary Fig. S6c). Regions that exhibited consistent and marked volumetric alteration in mutant monkeys were predominantly located in left visual area 1, left visual area 2, left anterior visual area, left ventral temporal cortex, and right medial frontal cortex.

To detect whether giant ANK2 depletion causes the core symptoms of ASDs, we performed a serial of behavioral tests including social interaction, environmental exploration, stereotypical behaviors, staying alone, and self-grooming⁶. Compared to the age- and gender-matched WT control monkeys, the mutant monkeys did not show typical ASDs-like behaviors. The frequencies and durations of both active and passive social interaction were comparable between WT and mutant monkeys (Fig. 1c).

Consistently, no obvious differences in exploration interests and stereotypes (Fig. 1d), as well as staying alone and self-grooming (Fig. 1e) were detected between mutant monkeys and WT controls. These data collectively suggest that giant ANK2 depletion in non-human primate does not cause ASDs-like behaviors. This is in sharp contrast to the observations in the mutant mice⁴.

Sleep is closely associated with neuroplasticity, brain development, and health. We wondered whether the brain defects in mutant monkeys could cause parahypnosis. The sleep–wake cycle was monitored at 9-month, 15-month, and 24-month by actigraphy, which is reliable to score the sleep state in monkeys¹¹. The results showed that mutant monkeys at each age had normal total sleep and relaxed sleep when compared to their WT counterparts (P -values > 0.05). Consistently, the proportion of relaxed sleep in total sleep did not differ between mutant and WT monkeys (Fig. 1f). We also evaluated the day-time activity, night-time activity, and the ratio of the day-time/night-time activity. Mutant monkeys did not display any difference from WT in these respects either (Fig. 1g). In order to explore whether the age affected sleep–wake cycles between the two groups, the data were further analyzed in separate 2 (groups: KO vs WT) \times 3 (age: 9-month, 15-month, and 24-month) repeated-measure ANOVAs, with age being the repeated-measure. No significant differences were observed in both sleep and activity patterns between the two groups (all P -values > 0.05).

In summary, specific depletion of giant ANK2 protein in monkeys did not induce nonsyndromic ASDs-like behaviors or sleep and activity pattern alterations. This finding does not support the loss of giant ANK2 as an ASDs factor. Unexpectedly, giant ANK2 depletion caused drastic brain structural alteration in all mutant monkeys. Thus, the functions of giant ANK2 are evolutionarily divergent between rodents and primates. In addition, four mutant monkeys with drastic loss of brain volume displayed normal basic brain functions. This was consistent with several previous reports on human cases. For instance, patients who underwent surgical removal of one hemisphere in childhood had normal intra-hemispheric connectivity, social responsiveness, full-scale intelligence quotient, psychomotor function, and executive control¹². Two persons having severe hydrocephalus and drastic brain volume loss also showed normal brain functions^{13,14}. On the other hand, our monkey models can be used to study the functional re-organization and plasticity of brains, for which the molecular mechanisms still remain elusive.

Acknowledgements

We thank Professor Vann Bennett in Duke University for suggestions and comments on the launch of this work and manuscript preparation, and Dr. Wei-Dao Zhang for performing the immunoblotting analysis. This work was

supported by the National Natural Science Foundation of China (U1702284, 31730037, 31771174, 31960178, 81941014, 81771387, 31800901), the Strategic Priority Research Program of Chinese Academy of Sciences (XDB02020003, XDB32060200, XDB32030000), the National Key R&D Program of China (2017YFC1310400, 2018YFC1313803, 2018YFA0801403), the Bureau of Frontier Sciences and Education, Chinese Academy of Sciences (QYZDJ-SSW-SMC005), the Key-Area Research and Development Program of Guangdong Province (2019B030335001), the Applied Basic Research Programs of Science and Technology Commission Foundation of Yunnan Province (2018FB053, 2019FA007), and Shanghai Municipal Science and Technology Major Project (No. 2018SHZDX05).

Author details

¹Key Laboratory of Animal Models and Human Disease Mechanisms, Chinese Academy of Sciences and Yunnan Province, Kunming Institute of Zoology, Chinese Academy of Sciences, Kunming, Yunnan, China. ²School of Basic Medical Sciences, Yunnan University of Chinese Medicine, Kunming, Yunnan, China. ³Precise Genome Engineering Center, School of Life Sciences, Guangzhou University, Guangzhou, Guangdong, China. ⁴Primate Facility, National Research Facility for Phenotypic & Genetic Analysis of Model Animals, and National Resource Center for Non-Human Primates, Kunming Institute of Zoology, Chinese Academy of Sciences, Kunming, Yunnan, China. ⁵Institute of Neuroscience, State Key Laboratory of Neuroscience, Chinese Academy of Sciences, Shanghai, China. ⁶State Key Laboratory of Genetic Resources and Evolution, Kunming Institute of Zoology, Chinese Academy of Sciences, Kunming, Yunnan, China. ⁷Kunming College of Life Science, University of Chinese Academy of Sciences, Kunming, Yunnan, China. ⁸CAS Center for Excellence in Brain Science and Intelligence Technology, Chinese Academy of Sciences, Shanghai, China. ⁹KIZ/CUHK Joint Laboratory of Bioresources and Molecular Research in Common Diseases, Kunming Institute of Zoology, Chinese Academy of Sciences, Kunming, Yunnan, China. ¹⁰School of Life Science and Technology, Shanghai Tech University, Shanghai, China. ¹¹Yunnan Key Laboratory of Animal Reproduction, Kunming Institute of Zoology, Chinese Academy of Sciences, Kunming, China. ¹²Center for Excellence in Animal Evolution and Genetics, Chinese Academy of Sciences, Kunming, Yunnan, China

Author contributions

X.-X.H., P.Z., X.-T.H., Z.W., and Y.-G.Y. designed and supervised the project. J.-K.Z. performed the CRISPR/Cas9 preparation and all genotyping. X.-C.H., L.-Z.Y., and X.L. generated knockout monkeys. Z.-F.H. and L.-B.L. took care of monkeys. D.-D.Q. performed all behavioral tests. X.-Y.S. and H.-Z.C. performed MRI scanning and data analyses. C.L. collected all tissue samples. W.-D.Z. performed immunoblotting analysis. P.Z., D.-D.Q., X.-Y.S., Z.W., J.-K.Z., X.-X.H., and Y.-G.Y. wrote the manuscript. All authors read and approved the final version of the manuscript.

Conflict of interest

The authors declare no competing interests.

Publisher's note

Springer Nature remains neutral with regard to jurisdictional claims in published maps and institutional affiliations.

Supplementary information The online version contains supplementary material available at <https://doi.org/10.1038/s41421-021-00336-4>.

Received: 10 April 2021 Accepted: 2 September 2021

Published online: 30 November 2021

References

- Constantino, J. N. & Charman, T. Diagnosis of autism spectrum disorder: reconciling the syndrome, its diverse origins, and variation in expression. *Lancet Neurol.* **15**, 279–291 (2016).
- Lord, C. et al. Autism spectrum disorder. *Nat. Rev. Dis. Prim.* **6**, 1–23 (2020).
- Kunimoto, M., Otto, E. & Bennett, V. A new 440-kD isoform is the major ankyrin in neonatal rat brain. *J. Cell Biol.* **115**, 1319–1331 (1991).

4. Yang, R. et al. ANK2 autism mutation targeting giant ankyrin-B promotes axon branching and ectopic connectivity. *Proc. Natl Acad. Sci. USA* **116**, 15262–15271 (2019).
5. Chang, S. W. et al. Neuroethology of primate social behavior. *Proc. Natl Acad. Sci. USA* **110**, 10387–10394 (2013).
6. Chen, Y. et al. Modeling Rett syndrome using TALEN-edited MECP2 mutant cynomolgus monkeys. *Cell* **169**, 945–955 (2017).
7. Liu, Z. et al. Autism-like behaviours and germline transmission in transgenic monkeys overexpressing MeCP2. *Nature* **530**, 98–102 (2016).
8. Zhao, H. et al. Altered neurogenesis and disrupted expression of synaptic proteins in prefrontal cortex of SHANK3-deficient non-human primate. *Cell Res.* **27**, 1293–1297 (2017).
9. Lv, Q. et al. Normative analysis of individual brain differences based on a population MRI-Based atlas of cynomolgus macaques. *Cereb. Cortex* **31**, 341–355 (2021).
10. Van Essen, D. C. Surface-based approaches to spatial localization and registration in primate cerebral cortex. *Neuroimage* **23**, S97–S107 (2004).
11. Qin, D.-D. et al. Potential use of actigraphy to measure sleep in monkeys: comparison with behavioral analysis from videography. *Zool. Res.* **41**, 437–443 (2020).
12. Kliemann, D. et al. Intrinsic functional connectivity of the brain in adults with a single cerebral hemisphere. *Cell Rep.* **29**, 2398–2407 (2019).
13. Feuillet, L., Dufour, H. & Pelletier, J. Brain of a white-collar worker. *Lancet* **370**, 262 (2007).
14. Lewin, R. Is your brain really necessary? *Science* **210**, 1232–1234 (1980).

Online Supplementary Materials

Materials and Methods

Animals

The cynomolgus monkey (*Macaca fascicularis*) and rhesus monkey (*Macaca mulatta*) facility in this study is accredited by AAALAC International. All experimental protocols were approved by the Institutional Animal Care and Use Committee (IACUC) of Kunming Institute of Zoology, Chinese Academy of Sciences. Throughout the experiment, the monkeys were housed in a controlled environment (temperature: $22 \pm 1^\circ\text{C}$, relative humidity: $50\% \pm 5\%$) with 12 hours light / 12 hours dark cycle (lights on at 07:00 a.m.). All animals were given commercial monkey diet twice a day with tap water ad libitum and were fed fruits and vegetables once daily. Routine veterinary care was provided by professional keepers and veterinarians during the entire process of experiments to ensure good health.

CRISPR/Cas9-mediated *ANK2* targeted editing in monkeys and genotyping

Superovulation, oocytes collection, intracytoplasmic sperm injection (ICSI), injection of CRISPR-Cas9 system, embryo transfer and pregnancy diagnosis were performed as previously described¹. Briefly, healthy female cynomolgus monkeys, ranging in age from 5 to 8 years old with regular menstrual cycles, were selected as oocyte donors for superovulation. The selected monkeys were intramuscularly injected with rhFSH (Recombinant Human FSH, Gonal F, Laboratories Serono) at the same time each day for 8 days and on the ninth day they were injected with rhCG (Recombinant Human Chorionic Gonadotropin alpha for Injection, Merck Serono). 32-35 hours after administration of rhCG, laparoscopy was used for oocyte collection. The collected oocytes were cultured in the pre-equilibrated maturation medium, and the metaphase II arrested oocytes were used to perform ICSI. The fertilization was confirmed for the presence of two pronuclei. The fertilized oocytes were injected with Cas9 mRNA (20 ng/ μL) and sgRNAs (10 ng/ μL or 20 ng/ μL for each sgRNA). Injected embryos were cultured in chemically defined protein-free hamster embryo culture medium-9 (HECM-9, Millipore) to allow embryo development. Cleaved embryos of high quality at the two-cell to blastocyst stage in high sgRNA concentration group were transferred into the oviduct of the matched surrogate recipient monkeys. Typically, three embryos were transferred into each surrogate, and the pregnancy diagnosis was firstly performed by ultrasonography on 20–30 days after transfer.

The tissues of aborted fetuses, including placenta, umbilical cord, brain, heart, kidney, liver, lung, muscle, skin and/or ovary, were collected and then quick frozen in liquid nitrogen. For survivors, the placenta, umbilical cord, ear skin fibroblasts and/or peripheral blood were collected. The collected tissues were digested in lysis buffer (10 mM Tris-HCl, 0.4 M NaCl, 2 mM EDTA, 1% SDS and 100 mg/ml Proteinase K). The genomic DNA was extracted from lysate by phenol-chloroform, and the *ANK2* mutations were identified by T7E1 cleavage assay with T7 Endonuclease (NEB) and Sanger sequencing. The primer pairs for amplifying sgRNA-targeted regions of the

ANK2 gene were listed in Supplementary [Table S2](#).

Deep sequencing of the sgRNA targeted region of *ANK2* for validation

To further validate and quantify the mutations introduced by Cas9/sgRNA, we performed a targeted sequencing of the sgRNA targeted region of *ANK2* by using the second-generation sequencing technologies (deep sequencing). We used genomic DNA isolated from peripheral blood samples of all five live monkeys and brain (T89 and T112) or liver (T114) tissues from dead monkeys with successful gene editing of *ANK2* as revealed by the TA-cloning sequencing. Briefly, targeted regions of *ANK2* were PCR amplified using primer pair ANK2-HTS-(1-17)-F and ANK2-HTS-R (Table S2) and were subjected to Illumina NovaSeq 6000 for high-throughput sequencing. Reads of individual sample from pool-sequencing were splitting by using Fastq-multx (V1.3.1)²; paired-end reads mapping was conducted by BWA (V0.7.17)³ and Samtools (V1.7)⁴, and frequency distributions of amplicon were analyzed by CRIPRESSO2 (V2.0.43)⁵.

Immunoblotting analysis of *ANK2* knockdown

Double-stranded siRNA specifically targeting human *ANK2* was ordered from GenePharma. The siRNA designs were list below: antisense, 5'-AUAAAUGAUAGUCGUCGCTT-3', and sense, 5'-GCGGACGACUAUCAUUUAUTT-3'. The siRNA was transfected into human 293T cells with Lipofectamine 2000 (Invitrogen, 11668-019). Knockdown efficiency was evaluated by immunoblotting analysis at 48 hours after transfection and was used as a control for showing the knockdown of *ANK2* isoform.

Human 293T cells with or without siRNA transfection and homogenized brain tissues from wild-type monkey and giant *ANK2* knockout monkey (T114) were lysed with RIPA lysis buffer (Beyotime, P0013B) for 20 min in ice. The supernatants were collected after centrifuging at 10000 g at 4 °C for 10 min and subject to immunoblotting blotting analysis. Membrane was incubated with *ANK2* antibody (Biolegend, MMS-5246, 1:1000 dilution) followed by incubation with secondary antibody (Thermo Fisher Scientific, 31430, 1:5000 dilution). Images were captured using a Protein SimpleFluorChem system.

Magnetic resonance imaging (MRI) scanning and quantification

A detailed description of MRI experiment can be found in our previous studies⁶⁻⁹. Briefly, the MRI data were acquired from a United Imaging UMR 790 3T scanner (Shanghai, China) using a 12-channel knee coil. Before each MRI scanning session, all monkeys were injected intramuscularly with atropine (0.05 mg/kg) and ketamine (5 mg/kg) and sodium pentobarbital (20 mg/kg). Anesthesia was maintained with the lowest possible concentration of sodium pentobarbital under the close supervision of experienced veterinarians. High-resolution T1-weighted anatomical images were acquired using an MPRAGE sequence (TR = 13010 ms; TE = 5600 ms; inversion time = 880 ms; flip angle = 8°; acquisition voxel size = 0.5 × 0.5 × 0.5 mm³). For each animal, the first acquired T1-weighted image was selected as a reference and the

remaining images from that animal were aligned to it and then averaged to obtain the motion-corrected images using FMRIB's Linear Image Registration Tool in FSL software (<http://www.fmrib.ox.ac.uk/fsl/>)¹⁰. We applied intensity bias correction for field inhomogeneity to each motion-corrected image using CMTK's (<http://nitrc.org/projects/cmtk/>) *mrbias* tool¹¹. Then, tissue segmentation of T1-weighted images into gray matter (GM), white matter (WM), and cerebrospinal fluid (CSF) was performed using FMRIB's Automated Segmentation Tool within FSL¹². A tissue-probability map of GM was generated to calculate the GM volume for individual brain region. Each GM map was registered to the brain atlas space of macaque monkey by nonlinear Diffeomorphic Anatomical Registration Through Exponentiated Lie Algebra (DARTEL)¹³ and then modulated to preserve the regional volumetric information of GM tissue within a voxel. This was done by multiplying the intensity value of each voxel in the segmented images by the Jacobian determinants (non-linear components only) that were derived from the spatial registration process. Afterwards, images were smoothed with a 2-mm isotropic Gaussian kernel. Thus, the tissue volumes of GM, WM, and CSF were calculated from the corresponding partial volume maps, and the total brain volume was calculated by summing up these three partial volume maps in the native space. Note that individual brain sizes were corrected for group comparison.

Measurement of sleep-wake cycle

The Actical Physical Activity Monitors (Respironics, Pennsylvania, U.S.A.) were used to monitor sleep-wake cycle of free-moving monkeys (*ANK2* KO monkeys and their age- and gender-matched WT control monkeys) for seven consecutive days at three ages¹⁴. The Actical monitor uses a single internal omni-directional accelerometer that senses motion in all direction, integrates the amplitude and frequency of detected motion and produces an electrical current varying in magnitude. Therefore, an increased intensity of motion produces an increase in voltage. Actical stores the activity data in the forms of activity counts.

The state of sleep was scored in 1-min epochs to describe the nighttime sleep^{14,15}. When the monkey was observed to exhibit less than three times of body or limb movement within 1 min, the sleep was scored. During relaxed sleep, the animals exhibited no body or limb movements. Meanwhile, the Actical monitors stored the daytime and nighttime activity data, and the ratio of daytime/nighttime activity was also analyzed.

Behavioral performance

The social interaction test was used to characterize behavioral performance in monkeys¹⁵. This test avoids the use of reward, and does not require extensive training of the animal, making it possible to observe the natural performance of behaviors. The most commonly used test is one-to-one interaction, in which one test monkey (the mutant or its age- and gender-matched WT monkey) is paired with one sociable monkey. The behaviors tested include active and passive social interaction; exploratory and stereotypical behaviors, as well as staying alone and self-grooming.

Active social interaction is defined as initiating a play, sharing toys, grooming for others, sitting together (within another monkey's arms' reach or in contact) etc., while passive social interaction is defined as receiving aforesaid social interactions from the sociable monkey. Explorative behaviors included tactile exploration of the cage or environments and oral exploration of the cage or environments, which can be used to reflect the monkey's interests¹⁶. The stereotypical behaviors are defined as repetitive and consistent actions with no apparent purposes, including pacing (repetitive, ritualized movement usually involving circling in the cage), digit sucking (sucking on a finger or toe), self-grasping (grabbing or holding onto part of their own body), rocking (a back and forth movement of the upper body with still feet), bouncing (jumping up and down on all four legs), cage shaking (any vigorous shaking of the cage), body spasms (a quick shake of the body), and lip-smacking (pursing the lips together and moving them to produce a smacking sound). The monkey is considered as staying alone when there is no other monkey within its arms' reach. Self-grooming is defined as cleaning or maintaining the individual's own body or appearance, which may be indicative of stereotypes. In our experiment, the tested monkeys were recorded once daily (an hour a day) for seven consecutive days. Each video-recording was scored simultaneously by three observers unaware of animal grouping. The observers calculated the frequency and duration of the specific behavior by manual starting and stopping the video under the condition that they all agreed on the classification of the observed behavior. The inter-rater correlation coefficient was found to be > 0.90 through SPSS statistical analysis after a period of training. The duration of each behavior was scored and statistically compared between the KO and WT monkeys.

Statistical analyses

Data analysis was conducted using the SPSS version 24.0 software package (SPSS, Chicago, IL, U.S.A.). The normality of the data was analyzed by Kolmogorov-Smirnov tests. We compared the MRI data of each mutant monkey with specie-specific standard brain atlas for rhesus macaque (F99) and cynomolgus macaque (Cyno162) after having segmented each monkey's brain into 94 sub-regions, instead of using species-matched WT controls as the standard brain atlas was constructed using more individuals^{17,18}. The sleep-wake data were analyzed in separate 2 (groups: KO versus WT) \times 3 (age: 9 months, 15 months and 24 months) repeated-measures ANOVAs, with age being the repeated-measure. One-way ANOVA was used to analyze the differences in ASDs-like behaviors between the KO and WT monkeys. The alpha level was set at $p = 0.05$. All p values were generated using two-sided tests and all the data were presented as the mean \pm SEM (standard error of the mean).

Supplementary Table S1. The information for genetically modified monkeys with giant ANK2 targeted-mutations and wild type control monkeys

Monkeys	Species	Gender	Delivery mode	Rearing pattern	Genotype	Mutation
T87	Cynomolgus monkey	Male	Natural delivery	Mother-rearing	<i>ANK2^{tm/tm}</i>	Frameshift
T88	Cynomolgus monkey	Female	Natural delivery	Mother-rearing	<i>ANK2^{tm/tm}</i>	Frameshift
T105	Rhesus monkey	Male	Natural delivery	Mother-rearing	<i>ANK2^{tm/tm}</i>	Frameshift
T111	Rhesus monkey	Female	C-section	Nursery/peer-reared	<i>ANK2^{tm/tm}</i>	Frameshift
T113	Rhesus monkey	Female	C-section	Nursery/peer-reared	<i>ANK2^{tm/tm}</i>	Missense
CWT1	Cynomolgus monkey	Male	Natural delivery	Mother-reared	<i>ANK2^{+/+}</i>	—
CWT2	Cynomolgus monkey	Male	Natural delivery	Mother-reared	<i>ANK2^{+/+}</i>	—
CWT3	Cynomolgus monkey	Male	Natural delivery	Mother-reared	<i>ANK2^{+/+}</i>	—
CWT4	Cynomolgus monkey	Female	Natural delivery	Mother-reared	<i>ANK2^{+/+}</i>	—
CWT5	Cynomolgus monkey	Female	Natural delivery	Mother-reared	<i>ANK2^{+/+}</i>	—
CWT6	Cynomolgus monkey	Female	Natural delivery	Mother-reared	<i>ANK2^{+/+}</i>	—
RWT7	Rhesus monkey	Male	Natural delivery	Mother-reared	<i>ANK2^{+/+}</i>	—
RWT8	Rhesus monkey	Male	Natural delivery	Mother-reared	<i>ANK2^{+/+}</i>	—
RWT9	Rhesus monkey	Male	Natural delivery	Mother-reared	<i>ANK2^{+/+}</i>	—
RWT10	Rhesus monkey	Female	C-section	Nursery/peer-reared	<i>ANK2^{+/+}</i>	—
RWT11	Rhesus monkey	Female	C-section	Nursery/peer-reared	<i>ANK2^{+/+}</i>	—
T89	Cynomolgus monkey	Female	C-section	Died at day 1	<i>ANK2^{tm/tm}</i>	Frameshift
T110	Rhesus monkey	Male	Natural delivery	Died at day 1	<i>ANK2^{tm/tm}</i>	Frameshift
T112	Rhesus monkey	Male	C-section	Died at day 15	<i>ANK2^{tm/tm}</i>	Frameshift
T114	Rhesus monkey	Female	C-section	Died at day 17	<i>ANK2^{tm/tm}</i>	Frameshift

Note: Five mutant monkeys (*ANK2^{tm/tm}*) were generated in this study, and eleven gender and age-matched wild-type (WT, *ANK2^{+/+}*) control monkeys were selected in accordance with the delivery mode of mutant monkeys. If the mutant monkeys were born by natural delivery, the matched WT monkeys were also born by natural delivery. The “CWT” represents the cynomolgus WT monkey, while the “RWT” represents the rhesus WT monkey.

Supplementary Table S2. Primer pairs for amplifying sgRNA-targeted regions of the *ANK2* gene

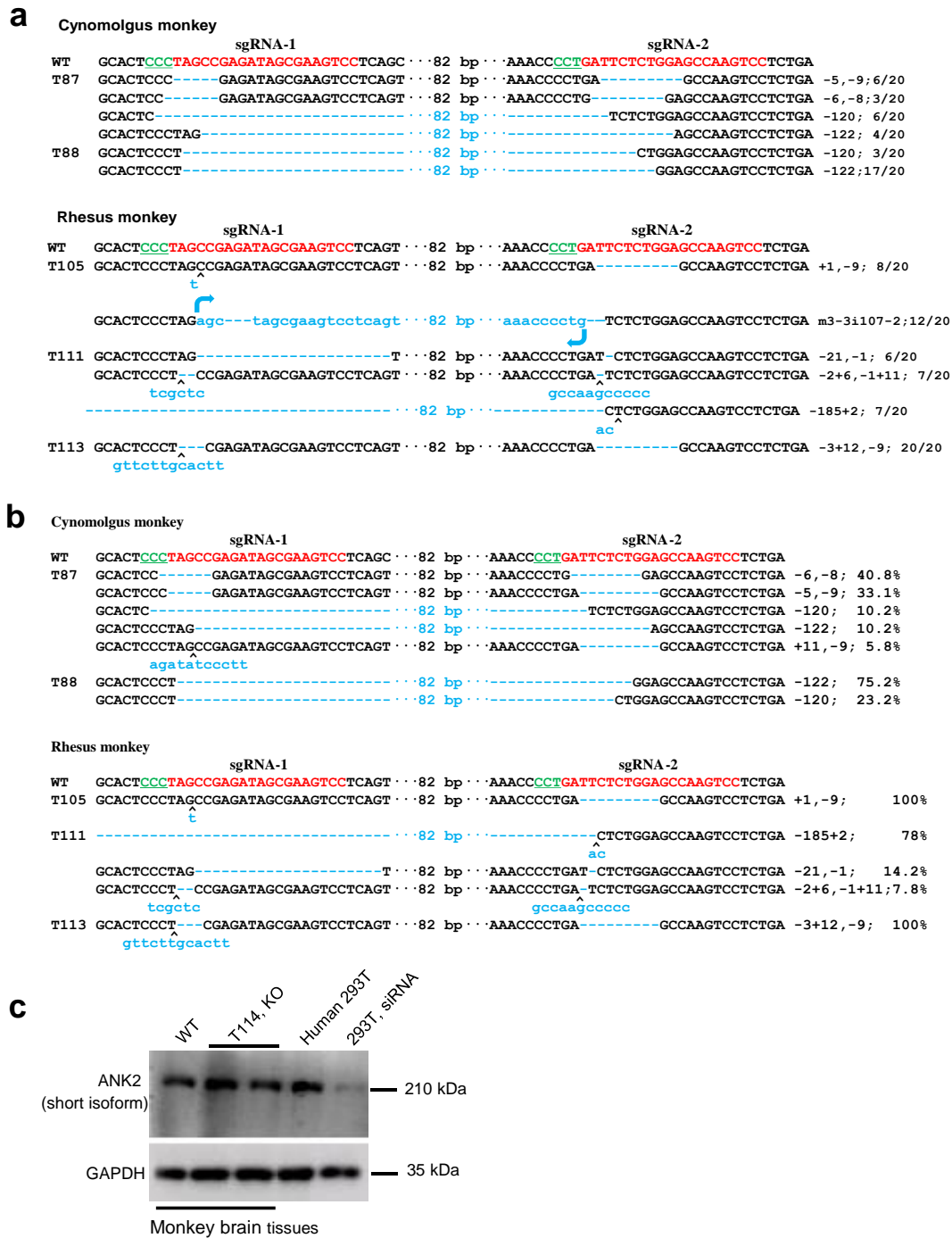
Name	Sequence (5'-3')	Amplicon	Sample
ANK2-1F	ACATTACTGGTGGCTCTGAAGA	723 bp	All
ANK2-1R	CTGCTCAAGACTGTCATCCTC		
ANK2-3F	AAGCACCTGCCTATGTCACCTT	2642 bp	All
ANK2-3R	CAATCTACTCGTGGAGATTCTGC		
ANK2-HTS1-F*	ACAGTGGAgacagatacaggaactgaatc	275 bp	T87
ANK2-HTS2-F	GCCAATCGgacagatacaggaactgaatc	275 bp	T88
ANK2-HTS3-F	ATGTCAGCgacagatacaggaactgaatc	275 bp	T89
ANK2-HTS4-F	CGATGTgacagatacaggaactgaatc	273 bp	CWT1
ANK2-HTS5-F	CTTGTAgacagatacaggaactgaatc	273 bp	CWT2
ANK2-HTS6-F	TGACCAAgacagatacaggaactgaatc	274 bp	CWT4
ANK2-HTS7-F	CAGATCTgacagatacaggaactgaatc	274 bp	CWT5
ANK2-HTS8-F	CCGTCCATgacagatacaggaactgaatc	275 bp	T105
ANK2-HTS9-F	AGTTCCTgacagatacaggaactgaatc	274 bp	T111
ANK2-HTS9L-F**	AGTTCCTctgtagtgtagcattagcta	454 bp for WT 271 bp for Mut	T111
ANK2-HTS10-F	GTAGAGCgacagatacaggaactgaatc	274 bp	T113
ANK2-HTS11-F	GTGGCCTgacagatacaggaactgaatc	274 bp	T110
ANK2-HTS12-F	CGTACGGgacagatacaggaactgaatc	274 bp	T112
ANK2-HTS12L-F	CGTACGGgaggtgccacagtcactgag	569 bp for WT 271 bp for Mut	T112
ANK2-HTS13-F	GAGTGGAGgacagatacaggaactgaatc	275 bp	T114
ANK2-HTS14-F	AGTCAAgacagatacaggaactgaatc	273 bp	RWT7
ANK2-HTS16-F	CACGATgacagatacaggaactgaatc	273 bp	RWT10
ANK2-HTS17-F	TCCCGAgacagatacaggaactgaatc	273 bp	RWT11
ANK2-HTS-R	ttcatctttggttcaacagg	-	-

* All ANK2-HTS-(1-17)-F primers are paired with ANK2-HTS-R primer.

** "L" labels forward primer for detecting samples of *ANK2* large deletion.

WT, wild type; Mut, mutant of *ANK2*

had a PCR product of 2642 bp in wild-type (WT) sample. The ANK2-3F/ANK2-3R primer pair amplified a larger region of *ANK2* compared to the ANK2-1F/ANK2-1R primer pair that yielded a product of 723 bp in WT sample. There was a large fragment deletion in embryo Mm #12. M, DNA ladder; WT, PCR products from respective wild-type cynomolgus and rhesus monkeys. Lower panel: Detection of Cas9/sgRNA-mediated cleavage of *ANK2* by T7EI cleavage assay. **(b)** Sanger sequencing results of modified *ANK2* alleles. Protospacers are in red text, while PAMs are in green and underlined. Mutations are in blue, and insertions (+), deletions (-) and point mutations (m) are shown on the right of each allele, with rates of clones for TA-sequencing. **(c)** Frequency of *ANK2*-edited embryos. The counts for genetically modified embryos are labelled on the top of each bar in the histogram, based on the Sanger sequencing results in **(b)**.



Supplementary Figure S2. Knockout of giant ANK2 in monkeys via the Cas9-mediated gene editing

(a-b) Sanger sequencing results (a) and deep sequencing results (b) of modified *ANK2* alleles in genetically modified monkeys. Genomic DNA isolated from peripheral blood samples was used for sequencing. Protospacers are in red text, PAMs are in green and underlined. Mutations are in blue, and insertions (+), deletions (-) and point mutations (m) are shown on the right of each allele. The rates of clones for TA-sequencing in (a) and percentage of high-throughput sequencing reads

in **(b)** are presented on the most right column in the respective figure section.

(c) The ANK2 protein expression in brain tissues of a wild-type (WT) monkey and giant ANK2 mutant rhesus monkey (T114, KO). Human 293T cells with or without ANK2 knockdown by siRNA were used as a control. The giant ANK2 protein could not be visible on the blot due to its large molecular weight for successful Western blot.

a Cynomolgus monkey

	sgRNA-1	sgRNA-2		
WT	GCACTCCCTAGCgaAGATAGCGAAGTCCTCAGT	AAACCCCTGATTTCTCTGGAGCCAAAGTCCTCTGA	82 bp	
T89 mutant	GCACTCCC-----GAGATAGCGAAGTCCTCAGT	AAACCCCTGAT-----CTGGAGCCAAAGTCCTCTGA		m2,-2; 5/15
Brain	GCACTCCC-----GAGATAGCGAAGTCCTCAGT	AAACCCCTGAT-----CTGGAGCCAAAGTCCTCTGA		-5,-3; 4/15
	GCACTCCCTAG-----GAGATAGCGAAGTCCTCAGT	TcCTCTG-AGCCAAAGTCCTCTGA		-114ml,-1;2/15
	GCATC-----GAGATAGCGAAGTCCTCAGT	TCTGGAGCCAAAGTCCTCTGA		-122; 4/15
Heart	GCACTCCCTAGCgaAGATAGCGAAGTCCTCAGT	AAACCCCTGATTTCTCTGGAGCCAAAGTCCTCTGA		m2,-2; 8/18
	GCACTCCC-----GAGATAGCGAAGTCCTCAGT	AAACCCCTGAT-----CTGGAGCCAAAGTCCTCTGA		m2,-3; 1/18
	GCACTCCCTAG-----GAGATAGCGAAGTCCTCAGT	TcCTCTG-AGCCAAAGTCCTCTGA		-114ml,-1;3/18
Kidney	GCACTCCC-----GAGATAGCGAAGTCCTCAGT	AAACCCCTGAT-----CTGGAGCCAAAGTCCTCTGA		-122; 1/18
	GCACTCCCTAGCgaAGATAGCGAAGTCCTCAGT	AAACCCCTGATTTCTCTGGAGCCAAAGTCCTCTGA		m2,-2; 4/16
	GCACTCCC-----GAGATAGCGAAGTCCTCAGT	AAACCCCTGAT-----CTGGAGCCAAAGTCCTCTGA		-5,-3; 6/16
Liver	GCACTCCCTAG-----GAGATAGCGAAGTCCTCAGT	TcCTCTG-AGCCAAAGTCCTCTGA		-114ml,-1;2/16
	GCATC-----GAGATAGCGAAGTCCTCAGT	TCTGGAGCCAAAGTCCTCTGA		-122; 5/16
	GCACTCCCTAGCgaAGATAGCGAAGTCCTCAGT	AAACCCCTGATTTCTCTGGAGCCAAAGTCCTCTGA		m2,-2; 5/15
Lung	GCACTCCC-----GAGATAGCGAAGTCCTCAGT	AAACCCCTGAT-----CTGGAGCCAAAGTCCTCTGA		-5,-3; 7/15
	GCACTCCCTAG-----GAGATAGCGAAGTCCTCAGT	TcCTCTG-AGCCAAAGTCCTCTGA		-114ml,-1;2/15
	GCATC-----GAGATAGCGAAGTCCTCAGT	TCTGGAGCCAAAGTCCTCTGA		-122; 1/15
Muscle	GCACTCCCTAGCgaAGATAGCGAAGTCCTCAGT	AAACCCCTGATTTCTCTGGAGCCAAAGTCCTCTGA		m2,-2; 10/15
	GCACTCCC-----GAGATAGCGAAGTCCTCAGT	AAACCCCTGAT-----CTGGAGCCAAAGTCCTCTGA		-5,-3; 2/15
	GCACTCCCTAG-----GAGATAGCGAAGTCCTCAGT	TcCTCTG-AGCCAAAGTCCTCTGA		-114ml,-1;3/15
Skin	GCACTCCCTAGCgaAGATAGCGAAGTCCTCAGT	AAACCCCTGATTTCTCTGGAGCCAAAGTCCTCTGA		m2,-2; 9/17
	GCACTCCC-----GAGATAGCGAAGTCCTCAGT	AAACCCCTGAT-----CTGGAGCCAAAGTCCTCTGA		-5,-3; 3/17
	GCACTCCCTAG-----GAGATAGCGAAGTCCTCAGT	TcCTCTG-AGCCAAAGTCCTCTGA		-114ml,-1;2/17
Ovary	GCATC-----GAGATAGCGAAGTCCTCAGT	TCTGGAGCCAAAGTCCTCTGA		-122; 3/17
	GCACTCCCTAGCgaAGATAGCGAAGTCCTCAGT	AAACCCCTGATTTCTCTGGAGCCAAAGTCCTCTGA		m2,-2; 3/17
	GCACTCCC-----GAGATAGCGAAGTCCTCAGT	AAACCCCTGAT-----CTGGAGCCAAAGTCCTCTGA		-5,-3; 6/17
Ovary	GCACTCCCTAG-----GAGATAGCGAAGTCCTCAGT	AAACCCCTGATTTCTCTGGAGCCAAAGTCCTCTGA		-9,-3; 1/17
	GCACTCCC-----GAGATAGCGAAGTCCTCAGT	TcCTCTG-AGCCAAAGTCCTCTGA		-114ml,-1;3/17
	GCATC-----GAGATAGCGAAGTCCTCAGT	TCTGGAGCCAAAGTCCTCTGA		-122; 4/17
Ovary	GCACTCCCTAGCgaAGATAGCGAAGTCCTCAGT	AAACCCCTGATTTCTCTGGAGCCAAAGTCCTCTGA		m2,-2; 8/18
	GCACTCCC-----GAGATAGCGAAGTCCTCAGT	AAACCCCTGAT-----CTGGAGCCAAAGTCCTCTGA		-5,-3; 5/18
	GCACTCCCTAG-----GAGATAGCGAAGTCCTCAGT	TcCTCTG-AGCCAAAGTCCTCTGA		-114ml,-1;2/18
GCATC-----GAGATAGCGAAGTCCTCAGT	TCTGGAGCCAAAGTCCTCTGA		-122; 3/18	

b Cynomolgus monkey

	sgRNA-1	sgRNA-2		
WT	GCACTCCCTAGCgaAGATAGCGAAGTCCTCAGT	AAACCCCTGATTTCTCTGGAGCCAAAGTCCTCTGA	82 bp	
T89 mutant	GCACTCCC-----GAGATAGCGAAGTCCTCAGT	AAACCCCTGAT-----CTGGAGCCAAAGTCCTCTGA		m2,-2; 45.6%
Brain	GCACTCCC-----GAGATAGCGAAGTCCTCAGT	AAACCCCTGAT-----CTGGAGCCAAAGTCCTCTGA		-5,-3; 43.1%
	GCACTCCCTAG-----GAGATAGCGAAGTCCTCAGT	TcCTCTG-AGCCAAAGTCCTCTGA		-114ml,-1; 5.8%
	GCATC-----GAGATAGCGAAGTCCTCAGT	TCTGGAGCCAAAGTCCTCTGA		-122; 5.5%

Supplementary Figure S3. Cas9/sgRNA-mediated ANK2 gene editing detected in diverse tissues from a dead cynomolgus monkey

(a) Sanger sequencing results of modified *ANK2* alleles in different tissues of a dead cynomolgus monkey (T89). PCR products were cloned into T-vector for sequencing. Protospacers are in red text, with PAM in green and underlined. Mutations are in blue, and insertions (+), deletions (-) and point mutations (m) are shown on the right of each allele, with rates of clones for TA-sequencing.

(b) High-throughput sequencing results of modified *ANK2* alleles in brain tissue of monkey T89.

a Rhesus monkey

	sgRNA-1	sgRNA-2		
WT	GCACTCCCTAGCCGAGATAGCGAAGTCCTCAGT	AAACCCTGATTCTCTGGAGCCCAAGTCCTCTGA	82 bp	
T110 mutant				
Brain	GCACTCCC-----GAGATAGCGAAGcCCTCAGT	AAACCCTG-----GAGCCAAGTCCTCTGA	82 bp	-5m1,-8
Kidney	GCACTCCC-----GAGATAGCGAAGcCCTCAGT	AAACCCTG-----GAGCCAAGTCCTCTGA	82 bp	-5m1,-8
Liver	GCACTCCC-----GAGATAGCGAAGcCCTCAGT	AAACCCTG-----GAGCCAAGTCCTCTGA	82 bp	-5m1,-8
Lung	GCACTCCC-----GAGATAGCGAAGcCCTCAGT	AAACCCTG-----GAGCCAAGTCCTCTGA	82 bp	-5m1,-8
Muscle	GCACTCCC-----GAGATAGCGAAGcCCTCAGT	AAACCCTG-----GAGCCAAGTCCTCTGA	82 bp	-5m1,-8
Skin	GCACTCCC-----GAGATAGCGAAGcCCTCAGT	AAACCCTG-----GAGCCAAGTCCTCTGA	82 bp	-5m1,-8
Spleen	GCACTCCC-----GAGATAGCGAAGcCCTCAGT	AAACCCTG-----GAGCCAAGTCCTCTGA	82 bp	-5m1,-8
T112 mutant				
Brain	GCACTCCCTAG-----	TCTCTGGAGCCCAAGTCCTCTGA	82 bp	-115+9; 17/20
	aacttgcaac			
	^			
	CGAGATAGCGAAGTCCTCAGT	AAACCCTG-TCTCTGGAGCCCAAGTCCTCTGA	82 bp	-306+8,-1;3/20
	ctctatatct			
Kidney	GCACTCCCTAG-----	TCTCTGGAGCCCAAGTCCTCTGA	82 bp	-115+9; 18/20
	aacttgcaac			
	^			
	CGAGATAGCGAAGTCCTCAGT	AAACCCTG-TCTCTGGAGCCCAAGTCCTCTGA	82 bp	-306+8,-1;2/20
	ctctatatct			
Liver	GCACTCCCTAG-----	TCTCTGGAGCCCAAGTCCTCTGA	82 bp	-115+9; 17/20
	aacttgcaac			
	^			
	CGAGATAGCGAAGTCCTCAGT	AAACCCTG-TCTCTGGAGCCCAAGTCCTCTGA	82 bp	-306+8,-1;3/20
	ctctatatct			
Lung	GCACTCCCTAG-----	TCTCTGGAGCCCAAGTCCTCTGA	82 bp	-115+9; 13/20
	aacttgcaac			
	^			
	CGAGATAGCGAAGTCCTCAGT	AAACCCTG-TCTCTGGAGCCCAAGTCCTCTGA	82 bp	-306+8,-1;7/20
	ctctatatct			
Muscle	GCACTCCCTAG-----	TCTCTGGAGCCCAAGTCCTCTGA	82 bp	-115+9; 18/20
	aacttgcaac			
	^			
	CGAGATAGCGAAGTCCTCAGT	AAACCCTG-TCTCTGGAGCCCAAGTCCTCTGA	82 bp	-306+8,-1;2/20
	ctctatatct			
Spleen	GCACTCCCTAG-----	TCTCTGGAGCCCAAGTCCTCTGA	82 bp	-115+9; 18/20
	aacttgcaac			
	^			
	CGAGATAGCGAAGTCCTCAGT	AAACCCTG-TCTCTGGAGCCCAAGTCCTCTGA	82 bp	-306+8,-1;2/20
	ctctatatct			
T114 mutant				
Kidney	GCACTCCC-----GAGATAGCGAAGTCCTCAGT	AAACCCT-----CTCTGGAGCCCAAGTCCTCTGA	82 bp	-5,-4; 3/20
	GCACTCCC-----GAGATAGCGAAGTCCTCAGT	AAAC-----AAGTCCTCTGA	82 bp	-5,-18; 8/20
	GCACTCCCTAG-----ATAGCGAAGTCCTCAGT	AAACCCTG-----GAGCCAAGTCCTCTGA	82 bp	-5,-8; 9/20
Liver	GCACTCCC-----GAGATAGCGAAGTCCTCAGT	AAACCCT-----CTCTGGAGCCCAAGTCCTCTGA	82 bp	-5,-4; 6/20
	GCACTCCC-----GAGATAGCGAAGTCCTCAGT	AAACCCTG-----GAGCCAAGTCCTCTGA	82 bp	-5,-8; 1/20
	GCACTCCC-----GAGATAGCGAAGTCCTCAGT	AAAC-----AAGTCCTCTGA	82 bp	-5,-18; 5/20
	GCACTCCCTAG-----ATAGCGAAGTCCTCAGT	AAACCCTG-----GAGCCAAGTCCTCTGA	82 bp	-5,-8; 8/20
Lung	GCACTCCC-----GAGATAGCGAAGTCCTCAGT	AAACCCT-----CTCTGGAGCCCAAGTCCTCTGA	82 bp	-5,-4; 2/20
	GCACTCCC-----GAGATAGCGAAGTCCTCAGT	AAAC-----AAGTCCTCTGA	82 bp	-5,-18; 10/20
	GCACTCCCTAG-----ATAGCGAAGTCCTCAGT	AAACCCTG-----GAGCCAAGTCCTCTGA	82 bp	-5,-8; 8/20
Muscle	GCACTCCC-----GAGATAGCGAAGTCCTCAGT	AAACCCT-----CTCTGGAGCCCAAGTCCTCTGA	82 bp	-5,-4; 4/20
	GCACTCCC-----GAGATAGCGAAGTCCTCAGT	AAAC-----AAGTCCTCTGA	82 bp	-5,-18; 10/20
	GCACTCCCTAG-----ATAGCGAAGTCCTCAGT	AAACCCTG-----GAGCCAAGTCCTCTGA	82 bp	-5,-8; 6/20
Skin	GCACTCCC-----GAGATAGCGAAGTCCTCAGT	AAAC-----AAGTCCTCTGA	82 bp	-5,-18; 7/20
	GCACTCCCTAG-----ATAGCGAAGTCCTCAGT	AAACCCTG-----GAGCCAAGTCCTCTGA	82 bp	-5,-8; 13/20
Spleen	GCACTCCC-----GAGATAGCGAAGTCCTCAGT	AAACCCT-----CTCTGGAGCCCAAGTCCTCTGA	82 bp	-5,-4; 2/20
	GCACTCCC-----GAGATAGCGAAGTCCTCAGT	AAAC-----AAGTCCTCTGA	82 bp	-5,-18; 8/20
	GCACTCCCTAG-----ATAGCGAAGTCCTCAGT	AAACCCTG-----GAGCCAAGTCCTCTGA	82 bp	-5,-8; 10/20

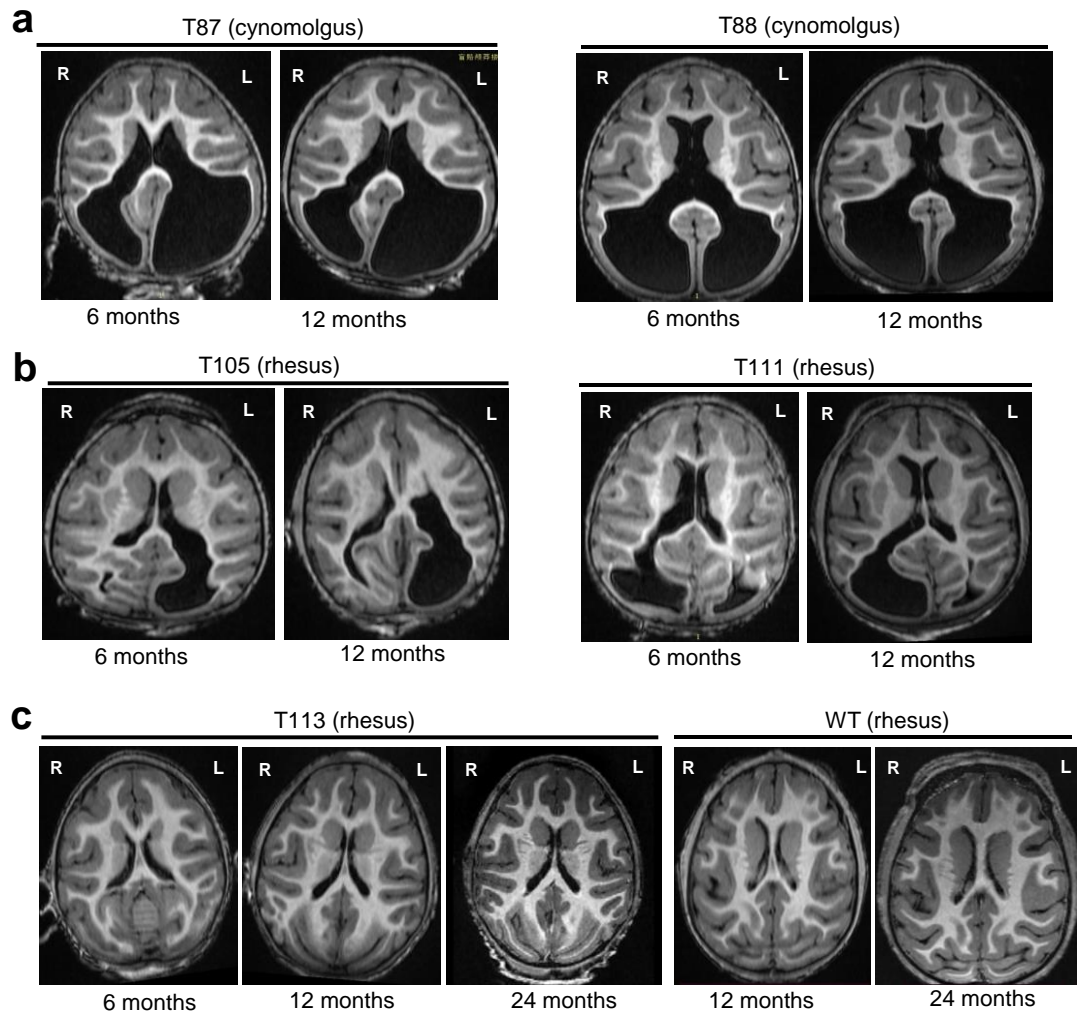
b Rhesus monkey

	sgRNA-1	sgRNA-2		
WT	GCACTCCCTAGCCGAGATAGCGAAGTCCTCAGT	AAACCCTGATTCTCTGGAGCCCAAGTCCTCTGA	82 bp	
T110 mutant				
Brain	GCACTCCC-----GAGATAGCGAAGcCCTCAGT	AAACCCTG-----GAGCCAAGTCCTCTGA	82 bp	-5m1,-8; 100%
T112 mutant				
Brain	GCACTCCCTAG-----	TCTCTGGAGCCCAAGTCCTCTGA	82 bp	-115+9; 52.3%
	aacttgcaac			
	^			
	CGAGATAGCGAAGTCCTCAGT	AAACCCTG-TCTCTGGAGCCCAAGTCCTCTGA	82 bp	-306+8,-1;47.7%
	ctctatatct			
T114 mutant				
Liver	GCACTCCCTAG-----ATAGCGAAGTCCTCAGT	AAACCCTG-----GAGCCAAGTCCTCTGA	82 bp	-5,-8; 51.2%
	GCACTCCC-----GAGATAGCGAAGTCCTCAGT	AAAC-----AAGTCCTCTGA	82 bp	-5,-18; 32.6%
	GCACTCCC-----GAGATAGCGAAGTCCTCAGT	AAACCCT-----CTCTGGAGCCCAAGTCCTCTGA	82 bp	-5,-4; 16.3%

Supplementary Figure S4. Cas9/sgRNA-mediated ANK2 gene editing detected in diverse tissues from dead rhesus monkeys

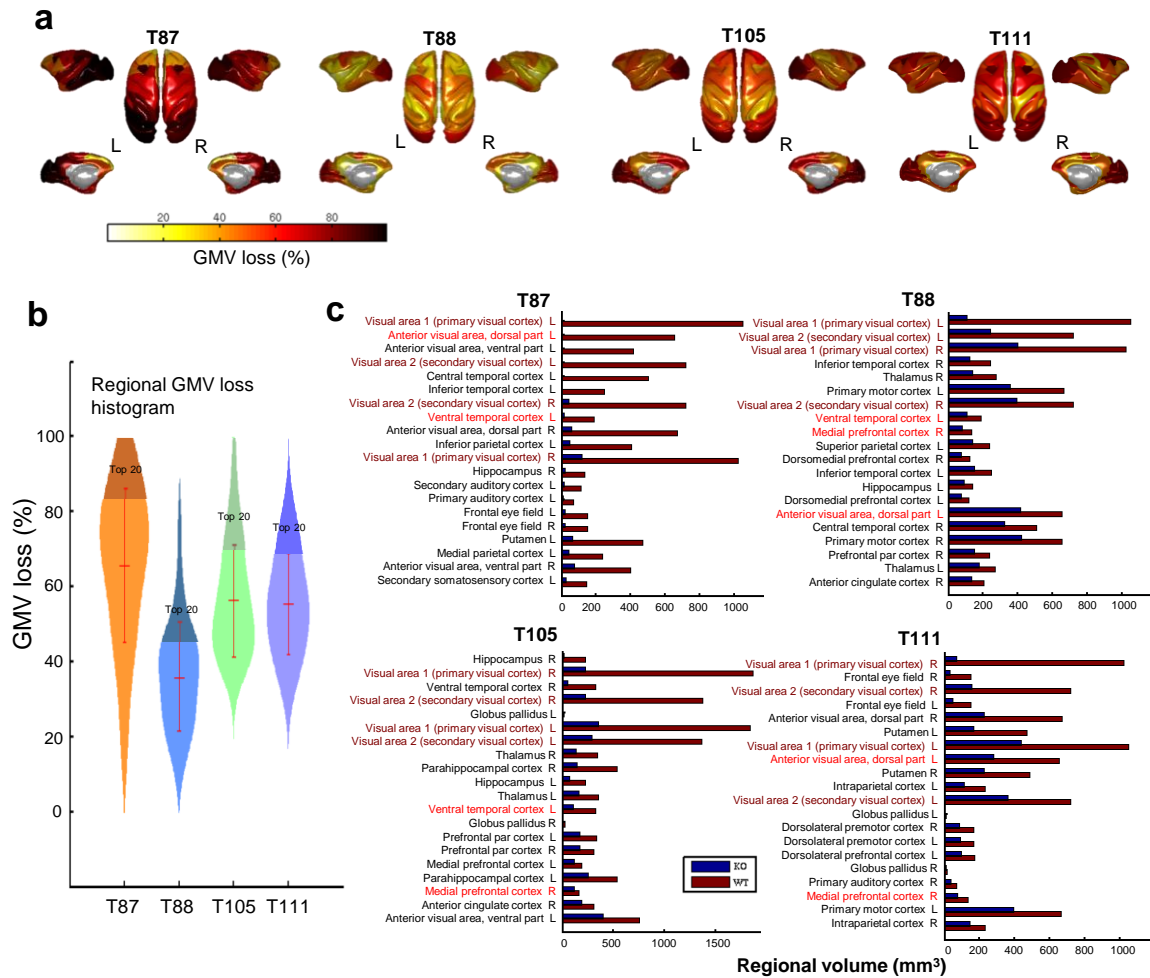
(a) Sanger sequencing results of modified *ANK2* alleles in different tissues of dead rhesus monkeys (T110, T112 and T114). PCR products were cloned into T-vector for sequencing. Protospacers are in red text, with PAM in green and underlined. Mutations are in blue, and insertions (+), deletions (-) and point mutations (m) are shown on the right of each allele, with rates of clones for TA-sequencing.

(b) High-throughput sequencing results of modified *ANK2* alleles in brain tissues of T110 and T112 and liver tissue of T114.



Supplementary Figure S5. MRI imaging showing brain volume loss in giant ANK2 knockout monkeys

(a-b) Example axial slices of structural images of cynomolgus monkeys (a: T87 and T88) and rhesus monkeys (b: T105 and T111) with giant ANK2 knockout (KO) at the ages of 6 and 12 months. (c) Example axial slices of structural images of rhesus monkey T113 and an age-matched wild-type (WT) rhesus monkey. Monkey T113 displayed grossly normal brain structure at all time-points examined. It has ANK2 mutations introduced by gene editing but the mutations may not significantly alter the function of giant ANK2.



Supplementary Supplementary Figure S6. Giant ANK2 knockout monkeys display reproducible brain volume loss

(a) Regional gray matter volume (GMV) loss for 94 brain regions was averaged across four KO monkeys and mapped on a standard monkey brain surface, in which the hot bar denotes the percentage of GMV loss.

(b) The overall distribution of the percentage of regional GMV loss in each KO monkey.

(c) Top 20 brain regions with the largest GMV loss are listed for each KO monkey compared to controls in the standard brain atlases. The horizontal axis represents the volume size of each brain region. Regions that exhibited consistent morphological changes in all four mutant monkeys are marked with dark red (light red for three mutant monkeys).

References

- 1 Chen, Y. *et al.* Functional disruption of the dystrophin gene in rhesus monkey using CRISPR/Cas9. *Human molecular genetics* **24**, 3764-3774 (2015).
- 2 Aronesty, E. Comparison of sequencing utility programs. *The open bioinformatics journal* **7**, 1-8 (2013).
- 3 Li, H. & Durbin, R. Fast and accurate short read alignment with Burrows–Wheeler transform. *Bioinformatics* **25**, 1754-1760 (2009).
- 4 Li, H. *et al.* The sequence alignment/map format and SAMtools. *Bioinformatics* **25**, 2078-2079 (2009).
- 5 Clement, K. *et al.* CRISPResso2 provides accurate and rapid genome editing sequence analysis. *Nat. Biotechnol.* **37**, 224-226 (2019).
- 6 Wang, Z. *et al.* The relationship of anatomical and functional connectivity to resting-state connectivity in primate somatosensory cortex. *Neuron* **78**, 1116-1126 (2013).
- 7 Lv, Q. *et al.* Large-Scale Persistent Network Reconfiguration Induced by Ketamine in Anesthetized Monkeys: Relevance to Mood Disorders. *Biol Psychiatry* **79**, 765-775 (2016).
- 8 Cai, D. C. *et al.* MECP2 Duplication Causes Aberrant GABA Pathways, Circuits and Behaviors in Transgenic Monkeys: Neural Mappings to Patients with Autism. *J Neurosci* **40**, 3799-3814 (2020).
- 9 Zhan, Y. F. *et al.* Diagnostic Classification for Human Autism and Obsessive–Compulsive Disorder Based on Machine Learning From a Primate Genetic Model. *Am J Psychiat* **178**, 65-76 (2021).
- 10 Jenkinson, M., Bannister, P., Brady, M. & Smith, S. Improved optimization for the robust and accurate linear registration and motion correction of brain images. *Neuroimage* **17**, 825-841 (2002).
- 11 Likar, B., Viergever, M. A. & Pernus, F. Retrospective correction of MR intensity inhomogeneity by information minimization. *IEEE Trans Med Imaging* **20**, 1398-1410 (2001).
- 12 Zhang, Y., Brady, M. & Smith, S. Segmentation of brain MR images through a hidden Markov random field model and the expectation-maximization algorithm. *IEEE Trans Med Imaging* **20**, 45-57 (2001).
- 13 Ashburner, J. A fast diffeomorphic image registration algorithm. *Neuroimage* **38**, 95-113 (2007).
- 14 Qin, D. D. *et al.* Potential use of actigraphy to measure sleep in monkeys: comparison with behavioral analysis from videography. *Zoological research* **41**, 437-443 (2020).
- 15 Chen, Y. *et al.* Modeling Rett syndrome using TALEN-edited MECP2 mutant cynomolgus monkeys. *Cell* **169**, 945-955 (2017).
- 16 Qin, D. *et al.* The first observation of seasonal affective disorder symptoms in Rhesus macaque. *Behavioural brain research* **292**, 463-469 (2015).
- 17 Lv, Q. *et al.* Normative analysis of individual brain differences based on a population MRI-based atlas of cynomolgus macaques. *Cerebral Cortex* **31**, 341-355 (2021).
- 18 Van Essen, D. C. Surface-based approaches to spatial localization and registration in primate cerebral cortex. *Neuroimage* **23**, S97-S107 (2004).